

Nature of seniority symmetry breaking in the semimagic nucleus ^{94}Ru

B. Das^{1,*}, B. Cederwall^{1,†}, C. Qi¹, M. Górska², P. H. Regan^{3,4}, Ö. Aktas¹, H. M. Albers², A. Banerjee², M. M. R. Chishti³, J. Gerl², N. Hubbard^{2,5}, S. Jazrawi^{3,4}, J. Jolie⁶, A. K. Mistry^{2,5}, M. Polettini^{7,8}, A. Yaneva^{2,6}, S. Alhomaidhi^{2,5}, J. Zhao², T. Arici², S. Bagchi⁹, G. Benzoni⁸, P. Boutachkov², T. Davinson¹⁰, T. Dickel^{2,11}, E. Haettner², O. Hall¹⁰, Ch. Hornung², J. P. Hucka⁵, P. R. John⁵, I. Kojouharov², R. Knöbel², D. Kostyleva², N. Kuzminchuk², I. Mukha², W. R. Plass^{2,11}, B. S. Nara Singh¹², J. Vasiljević¹, S. Pietri², Zs. Podolyák³, M. Rudigier⁵, H. Rösch⁵, E. Sahin^{2,5}, H. Schaffner², C. Scheidenberger², F. Schirru², A. Sharma¹³, R. Shearman⁴, Y. Tanaka², J. Vesić¹⁴, H. Weick², H. J. Wollersheim², U. Ahmed⁵, A. Algora^{15,16}, C. Appleton¹⁰, J. Benito¹⁷, A. Blazhev⁶, A. Bracco^{7,8}, A. M. Bruce¹⁸, M. Brunet³, R. Canavan^{3,4}, A. Esmaylzadeh⁶, L. M. Fraile¹⁷, G. Häfner^{19,6}, H. Heggen², D. Kahl¹⁰, V. Karayonchev⁶, R. Kern⁵, A. Korgul²⁰, G. Kosir¹⁴, N. Kurz², R. Lozeva¹⁹, M. Mikolajczuk^{20,2}, P. Napiralla⁵, R. Page²¹, C. M. Petrache¹⁹, N. Pietralla⁵, J.-M. Régis⁶, P. Ruotsalainen²², L. Sexton¹⁰, V. Sanchez-Temble¹⁷, M. Si¹⁹, J. Vilhena²³, V. Werner⁵, J. Wiederhold⁵, W. Witt⁵, P. J. Woods¹⁰ and G. Zimba²²

¹KTH Royal Institute of Technology, 10691 Stockholm, Sweden

²GSI Helmholtzzentrum für Schwerionenforschung GmbH, 64291 Darmstadt, Germany

³Department of Physics, University of Surrey, Guildford GU2 7XH, United Kingdom

⁴National Physical Laboratory, Teddington, Middlesex TW11 0LW, United Kingdom

⁵Institut für Kernphysik, Technische Universität Darmstadt, Darmstadt, Germany

⁶Institut für Kernphysik der Universität zu Köln, Zùlpicher Strasse 77, D-50937 Köln, Germany

⁷Dipartimento di Fisica, Università degli Studi di Milano, 20133 Milano, Italy

⁸INFN, Sezione di Milano, 20133 Milano, Italy

⁹Indian Institute of Technology, Dhanbad 826004, Jharkhand, India

¹⁰School of Physics and Astronomy, University of Edinburgh, Edinburgh EH9 3FD, United Kingdom

¹¹Justus Liebig University, 35390 Giessen, Germany

¹²SUPA, School of Computing, Engineering and Physical Sciences, University of the West of Scotland, PA1 2BE Paisley, United Kingdom

¹³Department of Physics, Indian Institute of Technology Ropar, Rupnagar-140 001, Punjab, India

¹⁴Jozef Stefan Institute, Jamova cesta 39, 1000 Ljubljana, Slovenia

¹⁵Instituto de Física Corpuscular, CSIC–Universidad de Valencia, E-46071 Valencia, Spain

¹⁶Institute for Nuclear Research (ATOMKI), Bem ter 18/c, H-4026 Debrecen, Hungary

¹⁷Grupo de Física Nuclear and IPARCOS, Universidad Complutense de Madrid, CEI Moncloa, E-28040 Madrid, Spain

¹⁸School of Computing Engineering and Mathematics, University of Brighton, BN2 4AT Brighton, United Kingdom

¹⁹Université Paris-Saclay, IJCLab, CNRS/IN2P3, F-91405 Orsay, France

²⁰Faculty of Physics, University of Warsaw, PL 02-093, Warsaw, Poland

²¹Department of Physics, Oliver Lodge Laboratory, University of Liverpool, Liverpool L69 7ZE, United Kingdom

²²University of Jyväskylä, Seminaarinkatu 15, 40014 Jyväskylä yliopisto, Finland

²³Laboratoire de Physique de la Matière Condensée et Nanostructures, Université Lyon I, CNRS, UMR 5586, Domaine scientifique de la Doua, F-69622 Villeurbanne Cedex, France



(Received 17 October 2021; revised 17 January 2022; accepted 11 March 2022; published 25 March 2022)

Direct lifetime measurements via γ - γ coincidences using a fast timing detector array consisting of $\text{LaBr}_3(\text{Ce})$ scintillators has been applied to determine the lifetime of low-lying states in the semimagic ($N = 50$) nucleus ^{94}Ru . The experiment was carried out as the first in a series of “FAIR-0” experiments with the DESPEC experimental setup at the Facility for Antiproton and Ion Research (FAIR). Excited states in ^{94}Ru were populated primarily via the β -delayed proton emission of ^{95}Pd nuclei, produced in the projectile fragmentation of an 850 MeV/nucleon ^{124}Xe beam impinging on a 4 g/cm² ^9Be target. While the deduced $E2$ strength for the $2^+ \rightarrow 0^+$ transition in the yrast cascade follows the expected behavior for conserved seniority symmetry, the intermediate $4^+ \rightarrow 2^+$ transition exhibits a drastic enhancement of transition strength in comparison with pure-seniority model predictions as well as standard shell model predictions in the fpg proton hole space with respect to doubly magic ^{100}Sn . The anomalous behavior is ascribed to a subtle interference between the wave function of the lowest

* Corresponding author: bdas@kth.se

† Corresponding author: bc@kth.se

seniority $\nu = 2$, $I^\pi = 4^+$ state and that of a close-lying $\nu = 4$ state that exhibits partial dynamic symmetry. In addition, the observed strongly prohibitive $6^+ \rightarrow 4^+$ transition can be attributed to the same mechanism but with a destructive interference. It is noted that such effects may provide stringent tests of the nucleon-nucleon interactions employed in state-of-the-art theoretical model calculations.

DOI: [10.1103/PhysRevC.105.L031304](https://doi.org/10.1103/PhysRevC.105.L031304)

Introduction. For any fermionic system, seniority, ν , is defined as the number of particles not in pairs coupled to angular momentum $J = 0$. It is a conserved quantum number for a system with n identical particles, each with angular momentum j , interacting through a pairing force [1]. Seniority symmetry has also been shown to be valid for a wider class of (short-range) empirical nucleon-nucleon interactions [2–4]. Seniority has a profound impact on nuclear structure near closed shells, e.g., via the occurrence of two-particle multiplets [5,6] and nuclear isomers [7], so called seniority isomers. Seniority can only be a strictly conserved quantum number for systems with $j \leq 7/2$. However, it has been demonstrated for a large number of different empirical interactions [8–12] that the typical seniority-mixing matrix elements are very small, of the order of tens of keV, even for systems with large j values. This gives rise to a few approximate symmetry rules, which can favorably be exploited in the interpretation of nuclear structure near closed shells [13]. The most important consequences of (approximate) seniority symmetry are (i) an independence of excitation energies on shell occupation n ; (ii) $\Delta\nu = 0$ matrix elements of even-tensor one- and two-particle operators are symmetric with respect to midshell, $n = (2j + 1)/2$ (except for a change of sign), where they vanish, creating long-lived isomers; (iii) $\Delta\nu = 2$ matrix elements of even-tensor one-body operators are symmetric to particle-hole (ph) conjugation with a maximum in midshell; and (iv) odd-tensor one- and two-particle operators are diagonal in seniority [14]. Deviations from good seniority in semimagic nuclei may be a result of mixing due to a seniority nonconserving interaction, proton-neutron interactions leading to core excitation across the shell gap, or by Landau-Zener mixing between close-lying levels [15,16]. Nuclei such as $^{94}_{44}\text{Ru}_{50}$ with valence particles situated in the upper half of the $N/Z = 28$ –50 major shell are influenced by the relative isolation of the $g_{9/2}$ subshell. The $j = 9/2$ system has received particular recent interest with respect to the exotic partial conservation of seniority [17–24]. That is, the seniority symmetry is partially conserved even though angular momentum $j = 7/2$ is the highest angular momentum for which a single- j shell can exhibit exact seniority symmetry. The partial symmetry restoration concerns, in particular, systems with four valence particles or holes isolated in a $j = 9/2$ system like $^{94}_{44}\text{Ru}_{50}$. Additional interest arises from the competition between seniority-conserving structures and configurations built from isoscalar spin-aligned proton-neutron pairs in self-conjugate spherical nuclei [25,26]

Experiment details and data analysis. The ^{95}Pd ions were produced by projectile fragmentation of a ^{124}Xe beam impinging on a 4 g/cm^2 ^9Be target after being accelerated to 850 MeV/nucleon by the SIS 18 synchrotron at the FAIR-GSI

Helmholtzzentrum für Schwerionenforschung accelerator facility, Darmstadt, Germany. Over a 3–5 second spill length the average primary beam current was $\approx 6 \times 10^8$ per second. The reaction products were separated according to their mass-to-charge ratio, A/Q , and the atomic number, Z , by the FRagment Separator (FRS) [27] using the $B\rho$ - ΔE - $B\rho$ and ToF- $B\rho$ - ΔE ion identification methods [28]. A total of $\approx 1.4 \times 10^7$ ^{95}Pd ions could be identified in this way over a six day beam period. The ions were transported to the S4 focal plane of the FRS and implanted in the Advanced Implantation Detector Array (AIDA) [29], composed of three double sided silicon strip detectors (DSSSDs). AIDA is situated at the center of the DEcay SPEctroscopy (DESPEC) setup [30], for the present experiment comprising a hybrid array of six triple cluster high-purity germanium (HPGe) detectors [31] and 36 LaBr₃(Ce) detectors of the FAst TIMing Array (FATIMA) [32]. In addition to implant and decay energies and positions, timing information was also obtained from AIDA and registered using a 64-bit 1 ns clock, known as the White Rabbit (WR) [33].

The 8^+ isomer in ^{94}Ru was populated primarily via the β -delayed proton decay from the $I^\pi = 21/2^+$ isomeric state in ^{95}Pd with a half-life of approximately 13 s [34]. Detection of β -delayed proton decays occurring within 42 s of a ^{95}Pd ion implantation in the same DSSSD pixel was used to initiate the measurement of time differences between γ rays recorded in FATIMA, as discussed in detail below. A time difference spectrum between the WR clocks attached to the FATIMA and the DSSSD setup, WRT, is shown in FIG. 1(a). By further applying a time window $25 \leq \text{WRT} \leq 200 \mu\text{s}$, the states populated following the β -delayed proton feeding of the 71 μs half-life [35] 8^+ isomer in ^{94}Ru could be cleanly selected. The 1431 keV ($2^+ \rightarrow 0^+$) coincidence condition on such events reveals the corresponding γ -ray cascade feeding the 2^+ state as shown in Fig. 1.

The β -delayed proton-selected γ - γ events recorded in FATIMA were used to extract the nuclear level lifetime information. To this end, all the FATIMA detectors were time aligned using the 344–779 keV delayed time distributions from ^{152}Eu source data, where the centroid of the time distribution [37],

$$C(D) = \frac{\int_{-\infty}^{\infty} tD(t)dt}{\int_{-\infty}^{\infty} D(t)dt}, \quad (1)$$

for each pair of detectors was calculated and combined. The aligned time difference spectra for all detectors can be seen in Fig. 2(a). The centroid for the antidelayered time distribution can be calculated in the same way to obtain the generalized centroid difference [38], ΔC , between the delayed and antidelayered time distributions. For a nuclear level with known

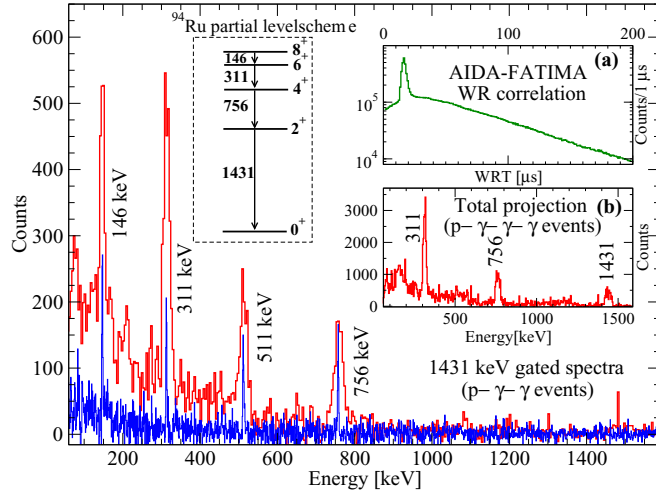


FIG. 1. Energy spectra gated on the 1431 keV transition from the β -delayed p - γ - γ events registered in the HPGe detectors (blue or deep grey) and the LaBr₃(Ce) detectors (red or light grey) are plotted with dispersions of 1 keV/channel and 4 keV/channel, respectively. The inset (a) shows the WR time correlation between AIDA and FATIMA. Inset (b) shows the total projection for γ -ray energies detected in the FATIMA detectors in coincidence with 146 keV registered in the HPGe detectors. The energies measured using the HPGe detectors agree within ± 0.5 keV with the previously reported values [36].

lifetime τ , the centroid difference between the delayed and antidelayed distributions contains the contribution from the lifetime and the prompt response of the setup [37] according to the expression

$$\begin{aligned} |\Delta C| &= \text{PRD} + 2\tau, & \Delta E_\gamma > 0, \\ &= \text{PRD} - 2\tau, & \Delta E_\gamma < 0, \end{aligned} \quad (2)$$

where ΔE_γ is the difference between the feeding and the decaying γ -ray energies for the level of interest and the prompt

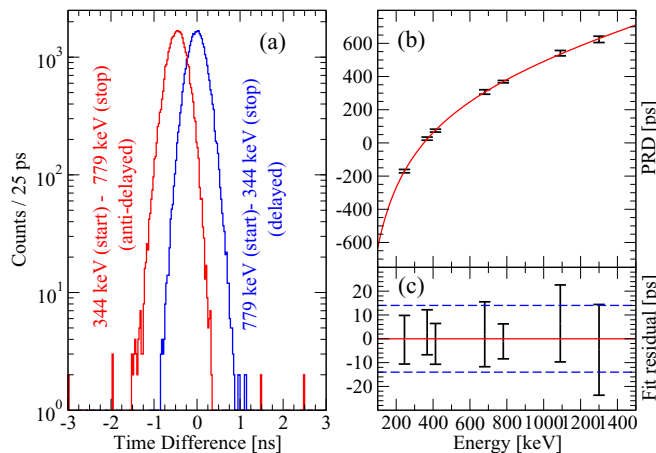


FIG. 2. (a) The delayed and antidelayed time distribution for the 344-779 keV coincident transitions of ^{152}Gd obtained from the β decay of a ^{152}Eu γ -ray source, (b) the PRD calibration curve, and (c) the fit residuals.

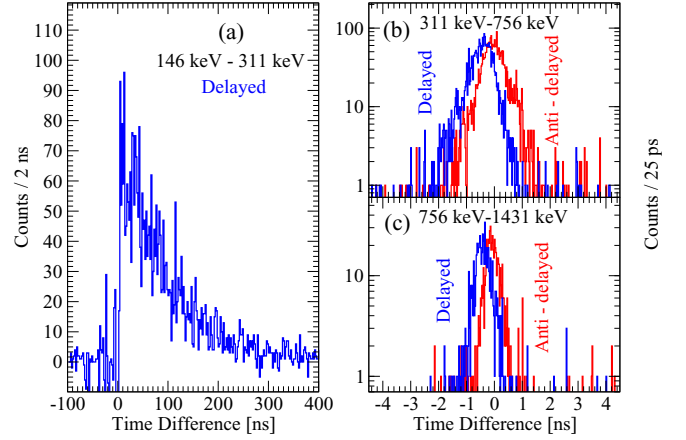


FIG. 3. (a) Background subtracted delayed time distribution for the 146-311 keV coincident transitions. Delayed and anti-delayed time distributions for 311-756 and 756-1431 keV coincidences are shown in panels (b) and (c), respectively.

response difference (PRD) is the energy dependent calibration to prompt radiation which was obtained using the various coincident transition pairs from a standard ^{152}Eu radioactive source. PRD values were adjusted to the reference energy 344 keV and fitted using the formula [39]

$$\text{PRD}(E_\gamma) = \frac{a}{\sqrt{b + E_\gamma}} + cE_\gamma + dE_\gamma^2 + e, \quad (3)$$

where a , b , c , d , and e are the parameters for the fit depicted in Fig. 2(b). The fit residuals in Fig. 2(c) help us to evaluate the uncertainty of the PRD calibration.

The lifetime of the 6^+ state was obtained from the delayed time distribution, $D(t)_{p1p2}$, using the 146 keV ($8^+ \rightarrow 6^+$) transition as the start signal and the 311 keV ($6^+ \rightarrow 4^+$) transition as the stop signal. The background contribution to the time distribution was corrected using the formula [40]

$$D(t) = D(t)_{p1p2} - D(t)_{p1bg2} - D(t)_{bg1p2} + D(t)_{bg1bg2}, \quad (4)$$

where the subscripts p and bg represent the peak and background of the start and stop signals, with the start (stop) signal indexed as 1 (2). The background corrected delayed time distribution obtained in this way is shown in Fig. 3(a), on which an exponential fit could be performed to obtain a lifetime value of $\tau(6^+) = 91(3)$ ns. This result agrees well with the previously reported value of $T_{1/2}(6^+) = 65(2)$ ns by Häusser *et al.* [41]. The lifetimes of the 4^+ and 2^+ states were measured using the generalized centroid difference (GCD) method [38]. Delayed and antidelayed timing spectra for (311,756) and (756,1431) keV coincidences are shown in Figs. 3(b) and 3(c), respectively. Here, the uncertainty in the experimentally obtained centroid difference, ΔC_{exp} , due to the background was corrected using the background correction factor [42]

$$t_{\text{cor}} = \frac{\Delta C_{\text{exp}} - \Delta C_{\text{BG}}}{P/B}, \quad (5)$$

where ΔC_{BG} is the centroid difference for the peak-background coincidence and P/B is the peak-to-background

TABLE I. Experimental mean lifetimes and $B(E2)$ strengths in ^{94}Ru in comparison with various shell model predictions. Experimental data except for $8^+ \rightarrow 6^+$ [41,45] are from the present work.

$I_i^\pi \rightarrow I_f^\pi$	τ (ps)	$B_{\text{EX}}(E2)$ ($e^2\text{fm}^4$)	$B_{\text{SMLB}}(E2)$ ($e^2\text{fm}^4$)	$B_{\text{SDGN}}(E2)$ ($e^2\text{fm}^4$)
$8^+ \rightarrow 6^+$	$102(4) \times 10^6$	0.09(1)	2.0	0.77
$6^+ \rightarrow 4^+$	$91(3) \times 10^3$	3.0(2)	6.1	17.3
$4^+ \rightarrow 2^+$	32(11)	103(24)	6.8	85.2
$2^+ \rightarrow 0^+$	≤ 15	≥ 10	225	295

ratio. The correction term was calculated for the decay transition background as well as the feeding transition background, to obtain a corrected centroid difference, ΔC_{FEP} [43],

$$\Delta C_{\text{FEP}} = \Delta C_{\text{exp}} + \frac{1}{2}[t_{\text{cor}}(\text{decay}) + t_{\text{cor}}(\text{feeder})]. \quad (6)$$

Values of $|\Delta C_{\text{FEP}}|$ obtained in this way are 474(22) ps, and 334(20) ps for the 4^+ and 2^+ states respectively. The absolute PRD values for the feeder-decay energy combination has been obtained from the PRD curve, and are 410(5) and 327(6) ps for the 4^+ and 2^+ states respectively. Finally using Eq. (2) we obtain the lifetime values $\tau(4^+) = 32(11)$ ps and $\tau(2^+) = 4(11)$ ps. The latter value translates to $\tau(2^+) \leq 15$ ps, the estimated experimental sensitivity limit. The results agree with the upper limits for these lifetimes previously measured by Mach *et al.* [20].

Discussion. While the energy spectrum of the ground-state band in ^{94}Ru up to $I^\pi = 8^+$ [36] exhibits the characteristic pattern of a seniority multiplet, the in-band $E2$ transition strengths reveal a somewhat different picture. Table I summarizes the experimental findings in comparison with the results of the shell model calculations reported by Mach *et al.* [20]. In this semimagic nucleus (number of neutrons $N = 50$) the proton Fermi level is situated near the middle of the $\pi g_{9/2}$ subshell where the seniority conserving $\nu = 2 \rightarrow \nu = 2$ transitions $8^+ \rightarrow 6^+$, $6^+ \rightarrow 4^+$, and $4^+ \rightarrow 2^+$ would be strongly suppressed in a situation with preserved seniority symmetry while the $\nu = 2 \rightarrow \nu = 0$ $2^+ \rightarrow 0_{\text{gs}}^+$ transition should have maximal strength. Interestingly, all the observed transition strengths except $B(E2 : 4^+ \rightarrow 2^+)$ follow this behavior. In addition to those $\nu = 0$ and $\nu = 2$ states, the four valence protons can form two additional pairs of $\nu = 4$, $J = 4$, 6 states within the partial seniority symmetry scheme mentioned above. The lowest-lying pair of these $\nu = 4$ states will never mix with the $\nu = 2$ states for systems isolated in the $g_{9/2}$ shell while the second pair of states is predicted to be much higher in excitation energy and therefore without influence on the observed spectrum. However, these $\nu = 4$ configurations are connected with the $\nu = 2$, 2^+ , and 4^+ states with strong $E2$ transitions and, notably, $B(E2 : 4^+, \nu = 4 \rightarrow 2^+, \nu = 2)$ is even larger than $B(E2 : 2^+, \nu = 2 \rightarrow 0_{\text{gs}}^+, \nu = 0)$ [22]. There is no contribution from the $g_{9/2}$ diagonal matrix elements to the seniority mixing, as discussed in Ref. [22]. On the other hand, the mixing between the partially seniority-conserved $\nu = 4$ configuration and the $\nu = 2$ configuration can be very sensitive to the strength of nondiagonal two-body interaction matrix elements, e.g., $V_{p_3/2 p_3/2 g_9/2 g_9/2}^{J=2}$, connecting the main $g_{9/2}$

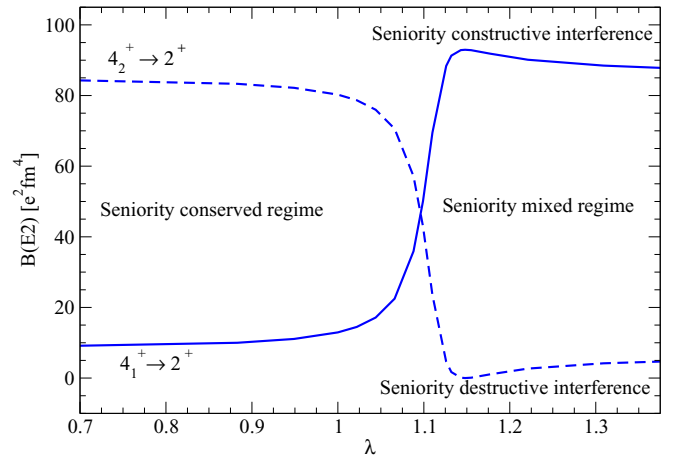


FIG. 4. Illustration of the influence of the nondiagonal matrix elements of the effective interaction on the $B(E2)$ strengths for transitions from the first (solid line) and second (dashed) 4^+ states to 2^+ ^{94}Ru in shell model calculations in the fpg space using the jun45 interaction [44]. The parameter λ is a renormalization factor scaling the effective interaction. A strong mixture between the $\nu = 2$ and 4 configurations, which can show drastically different constructive or destructive interferences, is expected when the effective interaction is slightly enhanced [22]. The result of a similar calculation for the particle-hole mirror nucleus ^{96}Pd is shown in Fig. 5 of Ref. [22]. See text for details.

components of the wave function with $p_{3/2}$ [22]. This is illustrated in Fig. 4 for the $4^+ \rightarrow 2^+$ transition in ^{94}Ru , where we simply multiplied this nondiagonal matrix element by a factor λ ($\lambda = 1$ corresponding to the original interaction). The rescaling of this interaction matrix element has quite limited influence on the energy spectra and wave functions of the low-lying yrast states. However, the wave functions of the $\nu = 4$, 4^+ , and 6^+ states have been shown to be very sensitive to such as renormalization due to the cancellation of the contribution from the diagonal matrix elements which usually dominate the nuclear properties. The renormalization effect leads to a quantum phase transitional behavior in a small window of the interaction strength and an enhancement of $B(E2 : 4_1^+ \rightarrow 2^+)$ due to the resulting seniority mixing. A similar sensitivity can be expected for the $6^+ \rightarrow 4^+$ transition as well as the corresponding transitions in the particle-hole mirror nucleus ^{96}Pd .

One can see clearly from the observed $B(E2 : 4_1^+ \rightarrow 2^+)$ values that the ^{94}Ru nucleus demonstrates constructive interference between the $\nu = 2$ and $\nu = 4$ configurations while the particle-hole mirror nucleus ^{96}Pd (corresponding to a system with four $g_{9/2}$ proton holes instead of the six $g_{9/2}$ proton holes) shows the opposite, destructive, behavior [20]. The amplitude of the mixing in these cases can be determined from the ratio between $B(E2 : 4^+, \nu = 4 \rightarrow 2^+)$ and $B(E2 : 2^+, \nu = 2 \rightarrow 0_{\text{gs}}^+)$. The same mechanism can therefore explain why the neighboring $N = 50$ isotones, ^{94}Ru and ^{96}Pd , which would be expected to exhibit exactly the same $B(E2)$ patterns if seniority symmetry is conserved, show so distinctly different $E2$ transition properties. Differently from the case of $B(E2 :$

$4^+ \rightarrow 2^+$), the $B(E2 : 6^+ \rightarrow 4^+)$ in ^{94}Ru is noticeably suppressed relative to standard model predictions (as represented by the ‘‘SMLB’’ prediction in Table I) and corresponds to a situation with destructive interference between the $\nu = 2$ and $\nu = 4$ configurations. Again, the situation is opposite for ^{96}Pd with a significant enhancement of $B(E2 : 6^+ \rightarrow 4^+)$ compared with standard seniority conserving calculations.

In Ref. [20] it was noticed that shell model calculations in two different model spaces using different Hamiltonians gave very different predictions of the $E2$ transition strengths of $N = 50$ isotones, and that a model space including core excited states was able to explain the observed seniority symmetry breaking effects. The sensitivity of the predicted quantities to small differences in the nondiagonal matrix elements for the applied effective interactions, which are rather unexpected, were then not considered. Contributions from energetic, cross-shell excitations due to the proton-neutron interactions are normally not expected to be significant for low-lying states in ^{94}Ru and neighboring nuclei. It might therefore be more natural to attribute the observed seniority symmetry breaking effects in ^{94}Ru and ^{96}Pd to the cross-diagonal components of the interaction within the same major shell rather than invoking excitations across the $N = 50$ shell gap. Although beyond the scope of the present work, it is noted that seniority symmetry breaking effects on $E2$ transition strengths could be used to test and to further develop the effective nucleon-nucleon interactions used in state-of-the-art nuclear models.

The $E2$ transition properties in nuclei $^{72,74}\text{Ni}$ observed recently [24], which are the neutron number analogs of ^{94}Ru and ^{96}Pd , can exhibit a similar feature of partial dynamic symmetry, though the ordering of the $\nu = 2$ and 4 states in the spectra may be different. It was suggested that the observed large deviations of experimental $E2$ transition rates from seniority-conserving predictions may be due to either configuration mixing with close-lying orbitals or to excitations across the $Z = 28$ and $N = 50$ shell gaps [24]. It is, however, likely that also the $\nu g_{9/2}$ system is subject to similar effects of interference between the $\nu = 2$ and $\nu = 4$ configurations as discussed for ^{94}Ru and ^{96}Pd above. Further measurements of the $E2$ transition properties of neutron rich nuclei near the $Z = 28$ and $N = 50$ closed shells could therefore help in pinning down details of, in particular, isospin dependent parts of the effective interactions.

Conclusions. In summary, lifetimes of low-lying excited states in ^{94}Ru have been measured using the fast timing

coincidence technique. The γ rays from the deexcitation of these states were detected in the FATIMA array of $\text{LaBr}_3(\text{Ce})$ scintillator detectors. The excited states in ^{94}Ru were populated in the β -delayed proton decay from the $I^\pi = 21/2^+$ isomeric state in ^{95}Pd [34], produced in the projectile fragmentation of a 850 MeV/nucleon ^{124}Xe beam impinging on a 4 g/cm² ^9Be target at the FAIR-GSI accelerator complex. The results show a good agreement between the measured lifetimes in the yrast cascade and the predictions of partial seniority conservation in standard shell model calculations within the *fpg* model space, with the notable exception of the 4^+ state. This is interpreted as resulting from constructive interference between the seniority $\nu = 2$ and $\nu = 4$ configurations of the same spin due to a small degree of seniority mixing induced by cross-orbital nondiagonal matrix elements of the nucleon-nucleon interaction within the *fpg* model space, i.e., without invoking cross-shell excitations. It is noted that a similar effect is predicted to be present in the neighboring $N = 50$ isotone and particle-hole mirror nucleus ^{96}Pd , although in that case the perturbation is caused by destructive interference between $\nu = 2$ and $\nu = 4$ configurations of the same spin. The results indicate that the observed phenomenon may be generalized to include also other regions of the nuclear chart and provide stringent tests of the nucleon-nucleon interactions employed in state-of-the-art configuration interaction models.

Acknowledgements. The authors would like to thank the staff of the FRS and the GSI accelerator, for their excellent support. This work was supported by the Swedish Research Council under Grants No. 621-2014-5558 and No. 2019-04880. Support by the STFC under Grants No. ST/G000697/1, No. ST/P005314, and No. ST/P003982/1; by the UK Department for Business, Energy and Industrial Strategy via the National Measurement Office; by the BMBF under Grants No. 05P19RDFN1 and No. 05P21RDFN1; by the Helmholtz Research Academy Hesse for FAIR (HFHF); by the GSI F&E Grant No. KJOLIE1820; and by BMBF grant 05P19PKFNA are also acknowledged. P.H.R. and R.S. acknowledge support from the National Measurement System program unit of the UK’s Department for BGS. G.H., M.S., and R.L. acknowledge IN2P3-GSI agreements, ADI-IDEX, and CSC-UPS grants. L.M.F. acknowledges the Spanish MICINN via Project No. RTI2018-098868-B-100. A.A. acknowledges partial support of the Ministerio de Ciencia e Innovacion Grant No. PID2019-104714GB-C21.

[1] G. Racah, *Phys. Rev.* **63**, 367 (1943).
 [2] G. Racah and I. Talmi, *Physica* **18**, 1097 (1952).
 [3] C. Schwartz and A. de Shalit, *Phys. Rev.* **94**, 1257 (1954).
 [4] A. de Shalit and I. Talmi, *Nuclear Shell Theory* (Academic, New York, 1963).
 [5] I. Talmi, *Simple Models of Complex Nuclei* (Harwood Academic, Chur, 1993)
 [6] P. Ring and P. Schuck, *The Nuclear Many Body Problem*, 3rd ed. (Springer, Berlin, 2004).

[7] D. H. Gloeckner, M. H. Macfarlane, R. D. Lawson, and F. J. D. Serduke, *Phys. Lett. B* **40**, 597 (1972).
 [8] R. Gross and A. Frenkel, *Nucl. Phys. A* **267**, 85 (1976).
 [9] R. D. Lawson, *Z. Phys. A* **303**, 51 (1981).
 [10] J. Blomqvist and L. Rydström, *Phys. Scr.* **31**, 31 (1985).
 [11] E. Caurier, M. Rejmund, and H. Grawe, *Phys. Rev. C* **67**, 054310 (2003).
 [12] L. Coraggio *et al.*, *J. Phys. G: Nucl. Part. Phys.* **26**, 1697 (2000).

- [13] R. F. Casten, *Nuclear Structure from a Simple Perspective* (Oxford University Press, Oxford, 2000).
- [14] J. J. Ressler, R. F. Casten, N. V. Zamfir, C. W. Beausang, R. B. Cakirli, H. Ai, H. Amro, M. A. Caprio, A. A. Hecht, A. Heinz, S. D. Langdown, E. A. McCutchan, D. A. Meyer, C. Plettner, P. H. Regan, M. J. S. Sziacchitano, and A. D. Yamamoto, *Phys. Rev. C* **69**, 034317 (2004).
- [15] L. D. Landau, *Physik. Z. Sowjet.* **2**, 46 (1932); L. D. Landau and E. M. Lifshitz, *Quantum Mechanics: Non-relativistic theory*, 3rd ed. (Pergamon, New York, 1977), pp. 342–351.
- [16] C. Zener, *Proc. R. Soc. London A* **137**, 696 (1932).
- [17] A. Escuderos and L. Zamick, *Phys. Rev. C* **73**, 044302 (2006).
- [18] P. Van Isacker and S. Heinze, *Phys. Rev. Lett.* **100**, 052501 (2008).
- [19] P. Van Isacker, *Int. J. Mod. Phys. E* **22**, 1330028 (2013).
- [20] H. Mach, A. Korgul, M. Gorska, H. Grawe, I. Matea, M. Stanoiu, L. M. Fraile, Y. E. Penionzkevich, F. D. Santos, D. Verney, S. Lukyanov, B. Cederwall, A. Covello, Z. Dlouhy, B. Fogelberg, G. DeFrance, A. Gargano, G. Georgiev, R. Grzywacz, A. F. Lisetskiy *et al.* *Phys. Rev. C* **95**, 014313 (2017).
- [21] C. Qi, *Phys. Rev. C* **83**, 014307 (2011).
- [22] C. Qi, *Phys. Lett. B* **773**, 616 (2017).
- [23] Y. Qian and C. Qi, *Phys. Rev. C* **98**, 061303(R) (2018).
- [24] A. I. Morales *et al.*, *Phys. Lett. B* **781**, 706 (2018).
- [25] B. Cederwall *et al.*, *Nature (London)* **469**, 68 (2011).
- [26] S. Zerguine and P. Van Isacker, *Phys. Rev. C* **83**, 064314 (2011).
- [27] H. Geissel *et al.*, *Nucl. Instrum. Methods Phys. Res., Sect. B* **70**, 286 (1992).
- [28] A. B. Garnsworthy *et al.*, *Phys. Rev. C* **80**, 064303 (2009).
- [29] C. J. Griffin *et al.*, *JPS Conf. Proc.* **14**, 020622 (2017).
- [30] B. Rubio, *Int. J. Mod. Phys. E* **15**, 1979 (2006).
- [31] M. Poletti *et al.*, *IL Nuovo Cimento* **44C**, 67 (2021).
- [32] M. Rudigier *et al.*, *Nucl. Instrum. Methods Phys. Res., Sect. A* **969**, 163967 (2020).
- [33] J. Serrano *et al.*, in *ICALEPCS 2009*, Proceedings of the International Conference on Accelerator and Large Experimental Physics Control Systems, Kobe, Japan, 2009 (ICALEPCS, Barcelona, 2009).
- [34] E. Nolte and H. Hick, *Phys. Lett. B* **97**, 55 (1980).
- [35] W. Kurcewicz, E. F. Zganjar, R. Kirchner, O. Klepper, E. Roeckl, P. Komminos, E. Nolte, D. Schardt, and P. Tidemand-Petersson, *Z. Phys. A* **308**, 21 (1982).
- [36] H. A. Roth *et al.*, *Phys. Rev. C* **50**, 1330 (1994).
- [37] J.-M. Régis, G. Pascovici, J. Jolie, and M. Rudigier, *Nucl. Instrum. Methods Phys. Res., Sect. A* **622**, 83 (2010).
- [38] J.-M. Régis *et al.*, *Nucl. Instrum. Methods Phys. Res., Sect. A* **726**, 191 (2013).
- [39] S. Ansari, J. M. Regis, J. Jolie, N. Saed-Samii, N. Warr, W. Korten, M. Zielinska, M. D. Salsac, A. Blanc, M. Jentschel, U. Koster, P. Mutti, T. Soldner, G. S. Simpson, F. Drouet, A. Vancraeynest, G. deFrance, E. Clement, O. Stezowski, C. A. Ur, W. Urban *et al.* *Phys. Rev. C* **96**, 054323 (2017).
- [40] E. R. Gamba, A. M. Bruce, and M. Rudigier, *Nucl. Instrum. Methods Phys. Res., Sect. A* **928**, 93 (2019).
- [41] O. Häusser, I. S. Towner, T. Faestermann, H. R. Andrews, J. R. Beene, D. Horn, and D. Ward, *Nucl. Phys. A* **293**, 248 (1977).
- [42] J.-M. Régis *et al.*, *Nucl. Instrum. Methods Phys. Res., Sect. A* **763**, 210 (2014).
- [43] J.-M. Régis, J. Jolie, N. Saed-Samii, N. Warr, M. Pfeiffer, A. Blanc, M. Jentschel, U. Koster, P. Mutti, T. Soldner, G. S. Simpson, F. Drouet, A. Vancraeynest, G. deFrance, E. Clement, O. Stezowski, C. A. Ur, W. Urban, P. H. Regan, Z. Podolyak, C. Larijani *et al.* *Phys. Rev. C* **95**, 054319 (2017).
- [44] M. Honma, T. Otsuka, T. Mizusaki, and M. Hjorth-Jensen, *Phys. Rev. C* **80**, 064323 (2009).
- [45] C. M. Lederer, J. M. Jaklevic, and J. M. Hollander, *Nucl. Phys. A* **169**, 449 (1971).